

Two-state model of conformational fluctuation in a DNA hairpin-loop

Liming Ying, Mark I. Wallace, David Klenerman *

Department of Chemistry, University of Cambridge, Lensfield Road, Cambridge CB2 1EW, UK

Received 22 August 2000; in final form 17 October 2000

Abstract

Stretched exponential kinetics have been observed in the conformational fluctuation of a DNA hairpin-loop under equilibrium conditions. In this paper, we employ a simple multiple-pathway two-state jump model to calculate single-molecule proximity ratio distributions. The simulation can reasonably reproduce the experimental single-molecule data of the conformational fluctuations in water, indicating that static disorder is dominant. In contrast, there exists significant discrepancy between the two-state simulation and experiment in buffer (2.5 mM *Tris*-HCl, 250 μ M EDTA, 100 mM NaCl), suggesting that both static and dynamic disorder may contribute to the non-exponential kinetics. © 2001 Elsevier Science B.V. All rights reserved.

1. Introduction

The hairpin-loop is a secondary structural motif frequently observed in both DNA and RNA where there is self-complementarity in the sequence. DNA hairpin-loops are involved in various biological functions, including gene expression and regulation [1]. Hairpin forming sequences have been found near the promoter region [2], enhancer binding site [3], receptor binding site [1] and in the origins of DNA replication [4]. Hairpin structure also exists in ligand-DNA aptamer complexes, which target cofactors, amino acids, peptides and proteins [5]. In addition, hairpin-loops were proposed as antisense drugs [6] and serve as DNA biosensors (e.g., molecular beacons) [7,8].

DNA hairpin structures fluctuate between different conformations and are generally classified as open or closed as shown in Fig. 1. Although the stability and thermodynamics of DNA hairpins have been investigated in detail [9], our understanding of the kinetics of loop-to-coil transitions remains very limited [10,11]. Recently, Bonnet et al. [12] examined the kinetics of conformational fluctuations in DNA hairpin-loops using a combination of fluorescence quenching and fluorescence correlation spectroscopy (FCS). A simple model of an all-or-none transition between open and closed states was supported by their experimental data. This model describes the open-to-closed transition as involving collision of the two arms of a hairpin, followed by the nucleation and the propagation of a base-paired region, whereas closed-to-open transition requires an energy fluctuation sufficiently large to unzip all the base pairs [12]. Statistical mechanical models have been proposed to describe the free energy cost of loop

* Corresponding author. Fax: +44-01223-336362.

E-mail address: dk10012@cam.ac.uk (D. Klenerman).

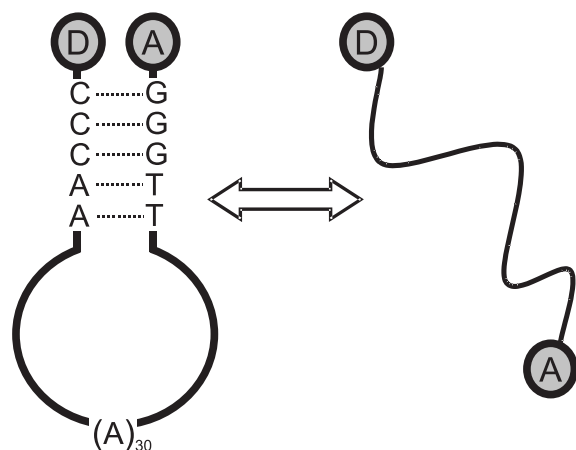


Fig. 1. Schematic of the donor and acceptor labelled DNA hairpin-loop. The DNA sequence is 5'-GGGTT(A)₃₀AACCCC'-3' with carboxytetramethylrhodamine (TMR) attached via a 6 carbon amino linker to the 3' end C' (modified cytosine), and Indodicarbocyanine (Cy5) attached via a 3 carbon amino linker at its 5' end. Five bases at the two ends are complementary to each other. DNA sample was purchased from Operon (Alameda, CA). The molecule is designed to fluctuate between open and closed states in solution at ambient temperature.

formation [13,14]. Ansari et al. [14] found the free energy cost of loop formation differs from that expected from entropy alone, and the free energy surface deviates from a strict all-or-none two-state transition.

Single-molecule spectroscopy has emerged as a powerful tool to explore the static and dynamic properties of biomolecules [15–20]. In this case, by attaching donor and acceptor fluorophores to a biological molecule, single-molecule FRET provides a method to probe conformational heterogeneity [16,21]. In a previous paper, we have observed submillisecond, non-exponential kinetics

for DNA hairpin-loop conformational fluctuations using fluorescence resonance energy transfer fluctuation spectroscopy (FRETfs) [22] under equilibrium conditions. We apply the kinetic parameters derived therein to a multiple-pathway two-state jump model. Based on this model, single-molecule proximity ratio distribution may be simulated and comparison can be made with experimental results.

2. Two-state model

Table 1 shows results of the stretched exponential fit and the mean relaxation time reported in our previous paper [22]. The stretched exponential of proximity ratio correlation function is defined as follows:

$$G(t) = G(0) \exp \left[- \left(\frac{t}{\tau} \right)^\beta \right], \quad (1)$$

where τ corresponds to the effective relaxation time associated with the correlated motion, and β is a stretch parameter that may be associated with the heterogeneity of the system. The mean relaxation time $\langle \tau \rangle$ can be related to τ and β by

$$\langle \tau \rangle = \int_0^\infty \exp \left[- \left(\frac{t}{\tau} \right)^\beta \right] dt = \left(\frac{\tau}{\beta} \right) \Gamma(\beta^{-1}), \quad (2)$$

where $\Gamma(\beta^{-1})$ is a gamma function.

The stretched exponential in Eq. (1) is only a phenomenological description of the kinetics and it is not sufficient to determine a particular mechanism for the conformational fluctuation. Both inhomogeneous kinetics (static disorder) and homogeneous kinetics (dynamic disorder) can lead to such non-exponential time dependence [23]. Since we observed well-separated sub-populations of

Table 1

Stretched exponential fit (Eq. (1)) to the auto-correlation function of proximity ratio for the conformational fluctuations of DNA hairpin-loop under three different conditions (Adopted from [22])

Conditions	$G(0)$	τ (ms)	β	$\langle \tau \rangle$ (ms)
MiliQ water	0.086	0.27	0.44	0.70
2.5 mM TE and 100 mM NaCl	0.056	0.19	0.46	0.45
2.5 mM TE, 100 mM NaCl and 2 μ M (T) ₃₀	0.022	0.32	0.54	0.57

DNA conformation in water in single-molecule measurement, we expect static disorder should dominate in this case.

In order to relate the phenomenological parameters to single-molecule experimental observations, we consider a two-state conformational fluctuation $A(\text{closed}) \rightleftharpoons B(\text{open})$ occurring in a system with static disorder. In addition, we assume that there is a large number of fluctuation pathways leading to the transformation of A to B and vice versa [24–26]. For a given pathway, we also assume that the two states can interconvert with simple first-order kinetics, and that the rate constant for jumping from closed state A to open state B is k_1 , jumping from open state B to closed state A is k_2 . Each pathway is characterised by a single relaxation rate constant, $k = k_1 + k_2$. Finally, we assume that the principle of detailed balance holds and therefore the ratio of forward and backward rates for each pathway is the equilibrium constant, K [26].

To analyse the single-molecule proximity ratio distribution, we first consider a simple one-pathway model and then extend it to multiple-pathway. A theoretical description of the one-pathway two-state dynamics of single biomolecules in solution was first given by Geva and Skinner [27]. Analytic expressions for the Fourier transforms of the probability densities for the amplitudes of the stochastic two-state jump model were derived. Subsequent work by Berezhkovskii et al. [28] has derived an explicit expression for the probability density of the amplitude. The equilibrium probabilities of occupation for the two states are defined as

$$p_1 = \frac{k_2}{k_1 + k_2} = \frac{k_2}{k}, \quad p_2 = \frac{k_1}{k_1 + k_2} = \frac{k_1}{k}. \quad (3)$$

Given the probability density that a molecule initially in state i spends a fraction x of time T in state 1 during the experimental measuring time T to be $P(x|T, i)$, when each single molecule measurement lasts the same amount of time T , the probability density of time fraction x is given by

$$P(x|T) = p_1 P(x|T, 1) + p_2 P(x|T, 2). \quad (4)$$

The explicit formula for $p(x|T, i)$ was derived as [28]

$$P(x|T, 1) = \delta(1-x) \exp(-p_2 k T) + p_2 k T \times \left\{ I_0(y) + \sqrt{\frac{p_1 x}{p_2(1-x)}} I_1(y) \right\} \times \exp\{-[p_2 x + p_1(1-x)]kT\} \quad (5)$$

and

$$P(x|T, 2) = \delta(x) \exp(-p_1 k T) + p_1 k T \times \left\{ I_0(y) + \sqrt{\frac{p_2(1-x)}{p_1 x}} I_1(y) \right\} \times \exp\{-[p_2 x + p_1(1-x)]kT\}, \quad (6)$$

where

$$y = 2kT \sqrt{p_1 p_2 x(1-x)}. \quad (7)$$

The delta functions are assumed to integrate to 1 when x is in the closed interval between 0 and 1. The $I_n(y)$ are modified Bessel functions of order n [29].

For a multiple pathway process, the distribution of kinetic rates is required to derive the probability density distribution. Provided that a fluctuation process occurs over a distribution of parallel activation energy barriers, a kinetic rate k can be associated with each pathway across the energy barrier. The distribution of activation energy barriers $\rho(E)$ can be equivalently described by the distribution of kinetic rates $\rho(k)$. These two distributions are related by [24]

$$\rho(k) = \left[-h \exp\left(\frac{E}{k_B T}\right) \right] \rho(E), \quad (8)$$

where E denotes the activation energy, T is the absolute temperature, h is the Plank constant, and k_B is the Boltzmann constant. If we assume that the complex kinetics are due to static disorder [25,26], the correlation function can be used to derive the distribution of kinetic rates [24,25]

$$\exp\left[-\left(\frac{t}{\tau}\right)^\beta\right] = \int_0^\infty \rho(k) \exp(-kt) dk. \quad (9)$$

For $\beta = 1/2$, this distribution can be expressed analytically [24,25,30],

$$\rho(k) = \frac{1}{2\sqrt{\pi\tau}} k^{-3/2} \exp\left(-\frac{1}{4k\tau}\right). \quad (10)$$

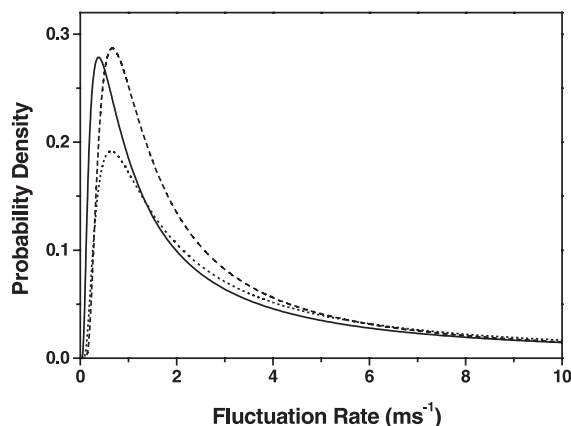


Fig. 2. The distributions of kinetic rates assuming static disorder in the activation energy barrier for the conformational fluctuations of DNA hairpin-loop under different conditions. Solid line: sample in water; dotted line: sample in 2.5 mM TE buffer with 100 mM NaCl; dashed line: sample in 2.5 mM TE buffer with 100 mM NaCl and 2 μM complementary strand (T)₃₀.

The distribution of rates can also be obtained numerically when $\beta \neq 1/2$ [24,30],

$$\rho(k) = \int_0^\infty \frac{1}{\pi} \exp \left[-kx - \left(\frac{x}{\tau} \right)^\beta \cos(\beta\pi) \right] \times \sin \left[\left(\frac{x}{\tau} \right)^\beta \sin(\beta\pi) \right] dx. \quad (11)$$

The distributions of fluctuation rates under three different experimental conditions are shown in Fig. 2 based on the parameters (τ and β) listed in Table 1.

The sum over all possible pathways characterised by rate constant k gives the total probability density distribution of state 1, $P_{\text{total}}(x)$

$$P_{\text{total}}(x) = \int_0^\infty P(x, k) \rho(k) dk, \quad (12)$$

where $P(x, k)$ is the probability density distribution of state 1 with kinetic rate k (which can be calculated using Eqs. (3)–(7)) and $\rho(k)$ is the probability density of k (which can be derived from Eq. (10) or (11)).

3. Results and discussion

Eq. (12) was used to simulate the probability density distributions of the time fraction spent in

the open state for hairpin molecules in pure water (Fig. 3A) and in buffer (2.5 mM *Tris*-HCl, 250 μM EDTA, 100 mM NaCl) (Fig. 3B). The simplest approximation for this open–closed transition is that there is no acceptor fluorescence in the open state, and no donor fluorescence in the closed state. The ratio of fluorescence intensity of two states can be approximated as 2 based on bulk fluorescence spectra (data not shown). Using these approximations the probability density distribu-

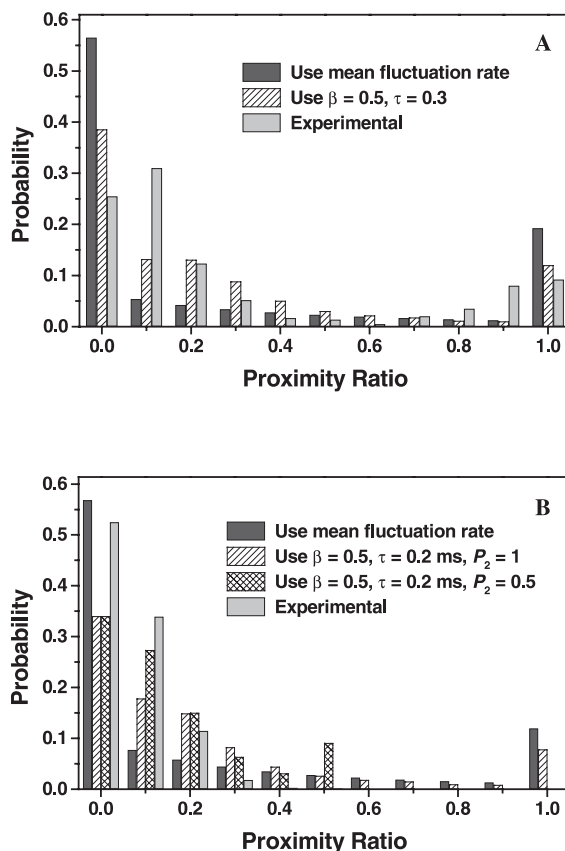


Fig. 3. Comparison of simulated and experimental proximity ratio distributions based on a two-state jump model. Panel (A) and (B) show results in MiliQ water and in 2.5 mM TE buffer with 100 mM NaCl, respectively. In panel A, all the simulations assume $p_1 = 0.3$, $P_1 = 0$, $P_2 = 1$. Dark grey: simulation using mean fluctuation rate; line hatched: simulation using $\beta = 0.5$, $\tau = 0.3$ ms; light grey: experimental data. In panel (B), all the simulations assume $p_1 = 0.25$, $P_1 = 0$. Dark grey: simulation using mean fluctuation rate; line hatched: simulation using $\beta = 0.5$, $\tau = 0.2$ ms, $P_2 = 1$; cross-hatched: simulation using $\beta = 0.5$, $\tau = 0.2$ ms, $P_2 = 0.5$; light grey: experimental data.

tions of time fraction x can be easily transformed to the proximity ratio density distributions according to $P_r = x/(2 - x)$. For convenience, we use Eq. (10) in the numerical integration of Eq. (12) as the β parameters are close to 1/2. Simulation results are shown in Fig. 3. Experimental single-molecule results are also given for comparison.

In pure water, the theoretical results give reasonable agreement with experiment. Distributed kinetic rates gave better fit to the experimental data than the mean rate. The major difference is in the sharp density peaks observed at both ends (0 and 1) of the proximity ratio in the simulation, these features being much broader for the experimental case. This broadening of the proximity ratio distribution may be simply due to photon shot noise [26]. This is supported by calculation of the standard deviation in proximity ratio based on a random distribution of both donor and acceptor signal, giving a standard deviation of 0.09 when the proximity ratio is either 0.1 or 0.9 [26]. Another contribution to the broadening may be that both open and closed states are actually present as an ensemble of slightly different sub-states with different proximity ratios.

In buffer, a significant discrepancy was found between all-or-none two-state model and experiment, indicating either another process is affecting the experimental distribution or more complicated fluctuation dynamics are present. The key difference is the complete absence of the population density for high proximity ratio. This is unexpected as the theoretical FRET efficiency from TMR-Cy5 pair in the completely closed state should be close to 100%. One possibility is that when the molecule forms rigid hairpin structure, the donor and acceptor are brought so close that fluorescence quenching in both donor and acceptor could occur [31]. However, no significant difference in the fluorescence intensity of samples in water and in buffer is observed when the acceptor is directly excited. Photobleaching can also be ruled out, as we see no change in correlation time when the excitation laser power is increased by a factor of 3. In fact, the hairpin structure may be quite loose (melting temperature of the hairpin-loop is about 12°C in 100 mM NaCl, whereas the experiment was performed at 18°C) and the aver-

age distance between donor and acceptor exceeds that expected from the fully closed state. For instance, if the closed state has a proximity ratio of 0.5 (equal donor and acceptor fluorescence), the proximity ratio distribution will be squeezed to $\{0, 0.5\}$ according to $P_r = x/(3 - x)$. This result is closer to, but still not an accurate description of the experimental data (see Fig. 3B).

There are two possible mechanisms for the deviation from two-state modelling. For transitions in which intermediate states are significantly populated, the conformational distribution will be broadened. The thermodynamics of open-to-closed transition of the hairpin-loop shows that in buffer/NaCl the transition is much less co-operative than that in water (unpublished results). Another possibility is that dynamic disorder of the fluctuation of DNA hairpin-loop in buffer/NaCl is significant. The dynamic distribution of the fluctuation rates may be substantially averaged out in our single-molecule measurement (0.5 ms time resolution), resulting in a broadened proximity ratio distribution and no sub-population can be resolved. In principle, experiments on individual immobilised DNA molecule can resolve both the static disorder and dynamic disorder, and this will be subject of our future study.

Since the two-state jump model can provide a reasonable description of the single molecule measurement of fluctuation of DNA hairpin-loop in water, a compact state must exist with a sizeable barrier connecting to the more open, random coiled state. On this evidence alone, it is impossible to tell if this closed state corresponds to a hairpin structure with some base pairs intact, or it is merely a collapsed structure (similar to molten globule in protein), where donor and acceptor are quite close (for example, 3 nm in distance should correspond to 97% FRET efficiency).

In our hairpin-loop design, hydrophobic interaction among bases in the oligonucleotide chain, in particular A–A stacking interaction is expected to contribute significantly in the enthalpy of conformational fluctuations. Goddard et al. [32] have estimated the enthalpy of destacking a single A–A pair to be ~ 2 kJ/mol. For poly(A) single-stranded DNA, we expect the effective roughness of the energy landscape to be around 6 kJ/mol (3 A–A

pairs), this will substantially reduce the effective intrachain diffusion coefficient. If the chain closing process starts from different stacked conformations in the loop or the first base pair forms at different position of the stem region of the hairpin, static disorder will be observed; on the other hand, if the stacked conformations interconvert quickly and the chain diffusion rate decreases as the collapse proceeds [33], then the non-exponential kinetics can be attributed to dynamic disorder. The discussions above only focus on the two-state model. More complicate models, (for example, a three-state model, i.e. a compact collapsed state separating the random coil state and the intact hairpin), are possible but beyond the limited scope of this study. We expect that further experiments and more accurate statistical mechanical models [14] may help to understand this issue.

Acknowledgements

We thank Professor Skinner and Dr. Geva for helpful discussions and referee's comments. This work was supported by the Leverhulme Trust (Grant #F65OE).

References

- [1] E. Zazopoulos, E. Lalli, D.M. Stocco, P. Sassone-Corsi, *Nature* (London) 390 (1997) 311.
- [2] X. Dai, M.B. Greizerstein, K. Nadas-Chinni, L.B. Rothman-Denes, *Proc. Natl. Acad. Sci. USA* 94 (1997) 2174.
- [3] C. Spiro, C.T. McMurray, *J. Biol. Chem.* 272 (1997) 33145.
- [4] K. Willwand, E. Mumtsidu, G. Kuntz-Simon, J. Rommelaere, *J. Biol. Chem.* 273 (1998) 1165.
- [5] C.H. Lin, W.M. Wang, R.A. Jones, D.J. Patel, *Chem. and Biol.* 5 (1998) 555.
- [6] J. Tang, J. Temsamani, S. Agrawal, *Nucleic Acids Res.* 21 (1993) 2729.
- [7] S. Tyagi, F.R. Kramer, *Nature Biotechnol.* 14 (1996) 303.
- [8] X. Liu, W. Tan, *Anal. Chem.* 71 (1999) 5054.
- [9] P.M. Vallone, T.M. Paner, J. Hilario, M.J. Lane, B.D. Faldasz, A.S. Benight, *Biopolymers* 50 (1999) 425.
- [10] J. Gralla, D.M. Crothers, *J. Mol. Biol.* 73 (1971) 497.
- [11] C.W. Hilbers, C.A. Haasnoot, S.H. de Bruin, J.J. Jorden, G.A. van der Marel, J.H. van Boom, *Biochimie* 67 (1985) 685.
- [12] G. Bonnet, O. Krichevsky, A. Libchaber, *Proc. Natl. Acad. Sci. USA* 95 (1998) 8602.
- [13] T.M. Paner, M. Amaratunga, M.J. Doktycz, A.S. Benight, *Biopolymers* 29 (1990) 1715.
- [14] S.V. Kuznetsov, Y. Shen, A.S. Benight, A. Ansari, Submitted to PNAS.
- [15] X.S. Xie, J.K. Trautman, *Ann. Rev. Phys. Chem.* 49 (1998) 441.
- [16] S. Weiss, *Science* 283 (1999) 1676.
- [17] H.P. Lu, L. Xun, X.S. Xie, *Science* 282 (1998) 1877.
- [18] L. Ying, X.S. Xie, *J. Phys. Chem. B* 102 (1998) 10399.
- [19] T. Ha, X. Zhuang, H.D. Kim, J.W. Orr, J.R. Williamson, S. Chu, *Proc. Natl. Acad. Sci. USA* 96 (1999) 9077.
- [20] Y. Jia, D.S. Talaga, W.L. Lau, H.S.M. Lu, W.F. DeGrado, R.M. Hochstrasser, *Chem. Phys.* 247 (1999) 69.
- [21] L. Ying, M.I. Wallace, S. Balasubramanian, D. Klenerman, *J. Phys. Chem. B* 104 (2000) 5171.
- [22] M.I. Wallace, L. Ying, S. Balasubramanian, D. Klenerman, *J. Phys. Chem. B* 104 (2000) 11551.
- [23] R. Metzler, J. Klafter, J. Jortner, M. Volk, *Chem. Phys. Lett.* 293 (1998) 477.
- [24] L.S. Liebovitch, T.I. Tóth, *Bull. Math. Biol.* 53 (1991) 443.
- [25] E. Rabani, J.D. Gezelter, B.J. Berne, *Phys. Rev. Lett.* 82 (1999) 3649.
- [26] M.O. Vlad, J. Ross, D.L. Huber, *J. Phys. Chem. B* 103 (1999) 1563.
- [27] E. Geva, J.L. Skinner, *Chem. Phys. Lett.* 288 (1998) 225.
- [28] A.M. Berezhkovskii, A. Szabo, G.H. Weiss, *J. Chem. Phys.* 110 (1999) 9145.
- [29] M. Abramowitz, I.A. Stegun, *Handbook of Mathematical Functions*, Dover, New York, 1971.
- [30] C.P. Lindsey, G.D. Patterson, *J. Chem. Phys.* 73 (1980) 3348.
- [31] J.L. Mergny, *Biochemistry* 38 (1999) 1573.
- [32] N.L. Goddard, G. Bonnet, O. Krichevsky, A. Libchaber, *Phys. Rev. Lett.* 85 (2000) 2400.
- [33] W.A. Eaton, V. Muñoz, S.J. Hagen, G.S. Jas, L.J. Lapidus, E.R. Henry, J. Hofrichter, *Ann. Rev. Biophys. Biomol. Struct.* 29 (2000) 327.